



Micromagnetics of anti-skyrmions in ultrathin films

Lorenzo Camosi, Nicolas Rougemaille, Olivier Fruchart, Jan Vogel, Stanislas Rohart

► To cite this version:

Lorenzo Camosi, Nicolas Rougemaille, Olivier Fruchart, Jan Vogel, Stanislas Rohart. Micromagnetics of anti-skyrmions in ultrathin films. 2017. hal-01662113v1

HAL Id: hal-01662113

<https://hal.science/hal-01662113v1>

Preprint submitted on 12 Dec 2017 (v1), last revised 12 Apr 2018 (v2)

HAL is a multi-disciplinary open access archive for the deposit and dissemination of scientific research documents, whether they are published or not. The documents may come from teaching and research institutions in France or abroad, or from public or private research centers.

L'archive ouverte pluridisciplinaire **HAL**, est destinée au dépôt et à la diffusion de documents scientifiques de niveau recherche, publiés ou non, émanant des établissements d'enseignement et de recherche français ou étrangers, des laboratoires publics ou privés.

Micromagnetics of anti-skyrmions in ultrathin films

Lorenzo Camosi,^{1,*} Nicolas Rougemaille,¹ Olivier Fruchart,^{1,2} Jan Vogel,^{1,†} and Stanislas Rohart³

¹*Univ. Grenoble Alpes, CNRS, Institut Néel, F-38000 Grenoble, France*

²*Univ. Grenoble Alpes, CNRS, CEA, Grenoble INP, INAC-SPINTEC, F-38000 Grenoble, France*

³*Laboratoire de Physique des Solides, Université Paris-Sud, CNRS UMR 8502, F-91405 Orsay Cedex, France*

We present a combined analytical and numerical micromagnetic study of the equilibrium energy, size and shape of anti-skyrmionic magnetic configurations. Anti-skyrmions and skyrmions are compared in systems with the same strength of magnetic interactions. Anti-skyrmions may be stabilized when the magnetic circular symmetry is broken due to the inversion of the chirality between perpendicular directions. Despite this symmetry breaking, if the dipolar interactions are neglected the skyrmion and the anti-skyrmion have the same energy and size. However, when dipolar interactions are considered, the energy of the anti-skyrmion is strongly reduced and its equilibrium size increased with respect to the skyrmion. This arises from the fact that both magnetic configurations are stable when the magnetic energies almost cancel each other, which means that a small variation of one parameter can drastically change their configuration, size and energy.

INTRODUCTION

The prediction [1, 2] and first experimental observations [3–7] of skyrmions has led to a huge increase of research on materials suitable for hosting this kind of structures. Skyrmions are chiral magnetic solitons, which can be stabilized by a chiral interaction like the Dzyaloshinskii-Moriya interaction (DMI) [8, 9] or by dipolar interactions. DMI is an anti-symmetric exchange interaction that favors perpendicular alignment between neighboring moments, which may exist in systems that lack a structural inversion symmetry. The presence of anisotropic DMI can stabilize anti-skyrmions [10, 11]. Skyrmions (SK) and anti-skyrmions (ASK) are characterized by their topological charge N_{sk} [12]. It yields to some of their most fascinating properties, such as the topological Hall effect [13, 14] or the skyrmion Hall effect [15–17]. In a continuous-field approximation N_{sk} can be written as the integral on the space (r, α) that counts how many times the magnetization $\mathbf{m}[\phi(\alpha), \theta(r)]$ wraps the unit sphere [12].

$$N_{\text{sk}} = \frac{1}{4\pi} \int \frac{d\theta}{dr} \frac{d\phi}{d\alpha} \sin \theta dr d\alpha = W \cdot p = \pm 1 \quad (1)$$

where θ and φ are the polar and azimuthal coordinates of \mathbf{m} (Fig. 1 and 2), p describes the direction of magnetization in the core of the moment texture [$p = 1$ (-1) if $\theta(r = 0) = 0$ (π)] and $W = [\phi(\alpha)]_{\alpha=0}^{\alpha=2\pi} / 2\pi = \pm 1$ is the winding number. Considering the same uniform magnetization, i.e. the same p value, SK ($\phi(\alpha) \propto \alpha$) and ASK ($\phi(\alpha) \propto -\alpha$) have opposite winding numbers and hence opposite topological charges.

SK have been observed both in bulk materials and thin films [3–7]. ASK have been observed in bulk materials [18], but not yet in thin film systems. The reason is that most thin film systems showing DMI studied until now were polycrystalline, leading to the same sign and strength of the DMI in any in-plane direction. In

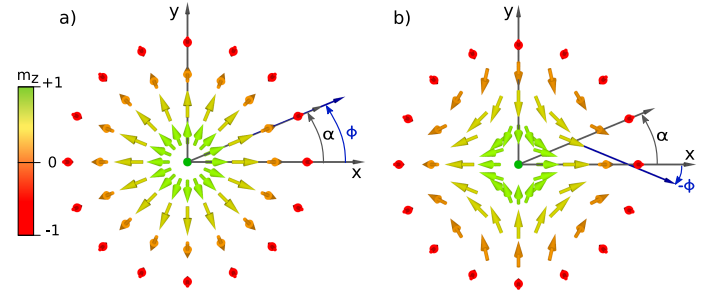


Figure 1: Sketch of the skyrmion and anti-skyrmion configurations. The illustration of α , the space angle in the plane, and ϕ , the in-plane magnetization angle, show the difference between a skyrmion ($\phi(\alpha) \propto \alpha$) and an anti-skyrmion ($\phi(\alpha) \propto -\alpha$).

order to stabilize ASK in thin films with perpendicular magnetization, the sign of DMI has to be opposite along two in-plane directions of the film. This may occur in epitaxial thin films with a C_{2v} symmetry [10, 11, 19]. For a Au/Co/W(110) thin film with C_{2v} symmetry, we have recently shown experimentally that the crystal symmetry can indeed give rise to an anisotropic DMI [10]. In this system, the DMI is a factor 2.5 larger along the $bcc[\bar{1}10]$ direction than along the $bcc[001]$ direction, but has the same sign. It was shown theoretically that an opposite sign of the DMI, needed for ASK, may be found for instance in a Fe/W(110) thin film [11].

The SK and ASK dynamics has already been theoretically investigated. If we consider the dynamics driven by spin-polarized currents, we can distinguish two main effects. The first is due to the different torques acting on the moment configurations, leading to a motion which keeps the same angle with respect to the current direction for SK, while it is strongly anisotropic for ASK

[20]. The second is given by the topological gyroscopic effect, also called skyrmion Hall effect [16, 17, 21]. In the same ferromagnetic state, the two magnetic configurations have opposite topological numbers, leading to opposite lateral deviations [22, 23]. The combination of the two effects leads to the suppression or enhancement of the ASK transverse motion depending on the current directions [20]. Moreover, the coupling of a SK and an ASK may lead to the absence of a skyrmion Hall effect [20].

A numerical micromagnetic study of the stability of SK and ASK in frustrated ferromagnets has been reported by Xichao et al. [24]. They evidenced the role of the dipolar interaction in the ASK stabilization. Our paper presents a complete combined analytical and numerical micromagnetic study of the equilibrium energy, size and shape of ASK in ferromagnetic thin films in the presence of anisotropic DMI. We point out the differences with the SK magnetic configuration. The paper is divided into two parts. In the first part we show that the micromagnetic energy of an ASK can be written in a circular symmetric form and that neglecting the dipolar interaction the ASK and the SK have the same equilibrium size and energy. In the second part we investigate the influence of the difference in dipolar energy on both the stability and the equilibrium sizes of SK and ASK.

ANTI-SKYRMIONS IN THE ABSENCE OF DIPOLAR COUPLING

It has been shown that skyrmionic configurations can be stabilized by DMI and/or dipolar interactions ([25–28]). For a small SK, the dipolar interaction can be neglected [29]. This is the case for SKs stabilized only by the competition between DMI, exchange and magnetic anisotropy [1]. In this part we develop micromagnetic calculations in order to study the energy and the size of SK and ASK configurations in absence of dipolar interaction. We focus on the simplest situation where the absolute value of the DMI is equal along the principal directions \mathbf{x} and \mathbf{y} but opposite in sign. Using the notation of the Lifshitz invariants $L_{jk}^{(i)} = m_j \frac{\partial m_k}{\partial i} - m_k \frac{\partial m_j}{\partial i}$ the micromagnetic DM energy can be written as :

$$E_{DMI} = t \iint D \left(L_{xz}^{(x)} - L_{yz}^{(y)} \right) dx dy \quad (2)$$

where m_x , m_y and m_z are the components of the unit magnetization vector \mathbf{m} and t is the film thickness. For simplicity, the exchange E_{ex} and magnetic anisotropy E_K energies are considered to be isotropic in the thin film plane (x, y) :

$$E_{ex} = t \iint A (\nabla \mathbf{m})^2 dx dy \quad (3)$$

with A the exchange constant and $(\nabla \mathbf{m})^2 = (\partial \mathbf{m} / \partial x)^2 + (\partial \mathbf{m} / \partial y)^2$, and

$$E_a = -t \iint K (\mathbf{m} \cdot \mathbf{e}_z)^2 dx dy \quad (4)$$

with K the out-of-plane anisotropy constant. In a local approximation, the effect of the dipolar interaction can be treated as an effective anisotropy $K_{\text{eff}} = K - \frac{1}{2} \mu_0 M_S^2$ in eq. (4). The DMI strongly depends on the in-plane magnetization whereas the anisotropy and the exchange do not, and therefore they are the same for a SK and an ASK of the same size.

The formulation of the complete micromagnetic energy for an arbitrary magnetization texture involves a large number of degrees of freedom. They can be strongly reduced using circular symmetry as it was done to solve the SK profile [25]. However the circular symmetry of ASK is broken by the presence on the chiral inversion. To approach this problem, we first consider a 1D modulation, propagating in an arbitrary direction in the plane. Then we use this result to solve the ASK 2D profile.

1D modulation

We consider a C_{2v} symmetry plane, where the DMI has opposite chirality along perpendicular direction ($D_x = -D_y$). In this system we introduce a 1D modulation propagating in a direction \mathbf{u} oriented by an angle α with respect to the x axis (Fig. 2).

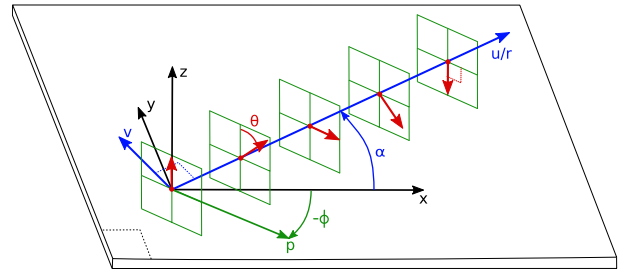


Figure 2: Frameworks used to describe a 1D modulation and 2D skyrmionic texture in a C_{2v} system

In the general case of isotropic DMI ($D_x = D_y$) the energy is an invariant upon in-plane framework rotation, whereas in our case the DMI takes more complex forms as a function of the framework orientation. Indeed in the rotated framework (\mathbf{u}, \mathbf{v}) , the integrated Dzyaloshinskii-Moriya interaction for the 1D modulation reads:

$$E_{DMI} = t \int \int D \left(\cos 2\alpha L_{uz}^{(u)} - \sin 2\alpha L_{vz}^{(u)} \right) dudv \quad (5)$$

This form promotes Néel type modulations with opposite chiralities for $\alpha = 0$ or $\pi/2$ and chiral Bloch type modulations for $\alpha = \pi/4$ and $3\pi/4$ [10]. During the modulation, the magnetization \mathbf{m} lies in the (p, z) plane, where p represents the modulation polarization (Fig. 2). It is therefore characterized by $\theta(u)$, the angle between $\mathbf{m}(u)$ and the z axis, and ϕ , the angle between \mathbf{p} and the x axis. The micromagnetic energy becomes :

$$E = Wt \int \left[A \left(\frac{d\theta}{du} \right)^2 - D \cos(\alpha + \phi) \frac{d\theta}{du} + K_{\text{eff}} \sin^2 \theta \right] du \quad (6)$$

where W is the width of the modulation and t is the film thickness.

Notice that the first (Heisenberg exchange, with exchange constant A) and third (effective magnetic anisotropy) terms do not depend on the propagation direction nor on the polarization. On the contrary, the Dzyaloshinskii-Moriya energy is strongly affected. Hence the polarization direction can be determined by minimizing the DMI term $-D \cos(\alpha + \phi)$. Therefore, for positive D (resp. negative), we find $\phi = -\alpha$ (resp. $\phi = -\alpha + \pi$). Such a relation exactly corresponds to the one requested for negative winding numbers (ASK). When this condition is fulfilled, the energy of the moment modulation can be formulated as a radial invariant. The micromagnetic energy of the 1D modulation becomes:

$$E = \int \left[A \left(\frac{d\theta}{du} \right)^2 - D \frac{d\theta}{du} + K_{\text{eff}} \sin^2 \theta \right] du \quad (7)$$

This indicates that for a given $\theta(u)$ the energy is isotropic. It means that an isotropic modulation ($\phi = \alpha$) in an isotropic environment ($D_x = D_y$) has the same energy than an anisotropic modulation ($\phi = -\alpha$) in an anisotropic environment ($D_x = -D_y$).

Micromagnetics of an anti-skyrmion

We extend the above calculation to a 2D texture. The texture is described by the two angles $\theta(r, \alpha)$ and $\phi(\alpha)$, defined as before, and where r and α are the circular coordinates in the (x, y) plane. Considering the result of the 1D investigation, the relation $\phi = -\alpha$ is kept. Therefore, the micromagnetic energy is isotropic, θ doesn't depend on α and the problem can be evaluated using a circular symmetry, with the energy

$$E = 2\pi t \int \left\{ A \left[\left(\frac{d\theta}{du} \right)^2 + \frac{\sin^2 \theta}{r^2} \right] - D \left[\frac{d\theta}{du} + \frac{\cos \theta \sin \theta}{r} \right] + K_{\text{eff}} \sin^2 \theta \right\} r dr \quad (8)$$

This equation is exactly the same as the one to describe a SK in a medium with isotropic DMI [1]. This means that, for a given set of A , D and K_{eff} , the ASK texture has a profile and an energy identical to a SK in an isotropic medium [1]. The only difference between the two configurations is the ϕ - α relationship; $\phi = \alpha$ for a SK ($W = 1$) and $\phi = -\alpha$ for an ASK ($W = -1$). In order to verify its validity we have performed micromagnetic simulations without dipolar interactions. We used an adaptation of the object-oriented micromagnetic framework code (OOMMF) [28, 30] including anisotropic DMI (see Fig. 3). The calculation is performed in a 400-nm diameter, 1-nm thick circular dot with typical magnetic parameters for systems where isolated skyrmions have been experimentally observed ($A = 16$ pJ/m, $K_{\text{eff}} = 0.2$ MJ/m³ and $D = 2$ mJ/m²) [7]. Comparing SK and ASK obtained respectively with $D_x/D_y = 1$ and -1 , identical energies and out-of-plane profiles are found. The ϕ - α relationship is confirmed validating the different assumptions in our model (in particular the hypothesis that ϕ is independent on r).

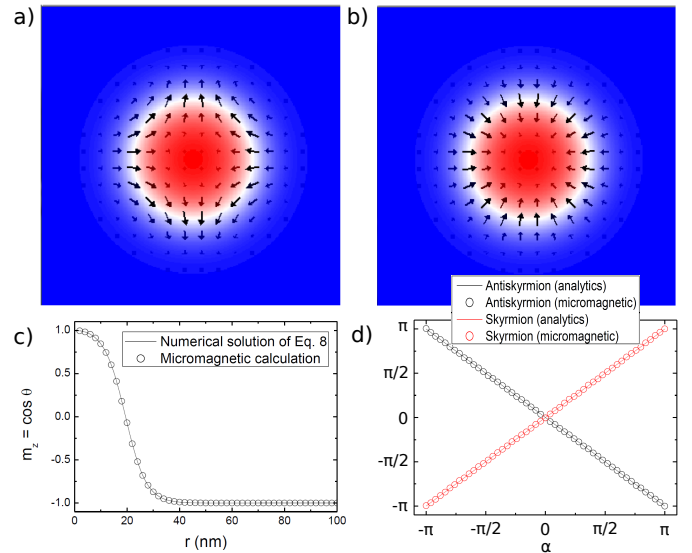


Figure 3: Comparison between analytical model and micromagnetic simulations. Spin map for an antiskyrmion (a) and a skyrmion (b). The arrows represent the in-plane magnetization and the color code the out-of-plane magnetization (red = up, white = in-plane and blue = down). (c) Comparison of the out-of-plane profile obtained with Eq. 8 and micromagnetic simulations. The profile of the SK and ASK are exactly the same. (d) ϕ - α relationship for SK and ASK.

ROLE OF DIPOLAR COUPLINGS

Determining the role of dipolar interactions on the stabilization of SK with micromagnetic analytical calculations is particularly difficult. This interaction has often

been neglected [25–28] or analytically expressed under approximations [31–33]. The two-fold symmetry of the ASK magnetic configuration does not allow to use a circular symmetry increasing the difficulty of this approach. Thus, we performed a study of the dipolar interaction effects on the SK and ASK configurations with the support of micromagnetic simulations using OOMMF [30] with an anisotropic DMI. For stabilizing SK and ASK in absence of an external magnetic field, we confine them into circular dots of 400 nm diameter, 1 nm thickness and mesh size of 1 nm.

Phenomenology of dipolar interactions

The effect of the dipolar interaction on the size and stability of SK and ASK in a dot can be phenomenologically understood considering the contributions from the surface and volume charges.

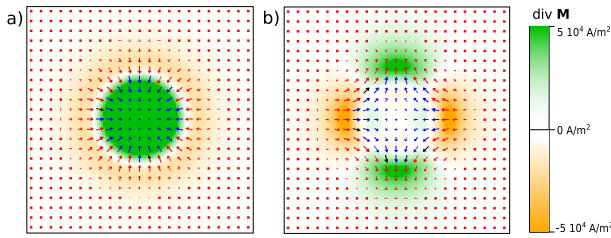


Figure 4: Representation of the volume charges ($\nabla \mathbf{m}$) for a skyrmion (a) and an anti-skyrmion (b) over the magnetic configuration (red arrows). The magnetic configurations are stabilized in an infinite film without the application of an external magnetic field with $M_s = 5 \cdot 10^5$ A/m $A_{\text{ex}} = 16$ pJ/m $K_{\text{eff}} = 200$ kJ/m³ $D = 2.0$ mJ/m². Isotropic DMI ($D_x = D_y$) allows the stabilization of a skyrmion whereas anisotropic DMI ($D_x = -D_y$) an anti-skyrmion.

Magnetic surface charges arise from the singularities of the magnetization divergence on the system surface. The texture core and the surrounding display opposite charge signs. The dipolar interaction reduces its energy when the magnetic flux closes [7, 32]. Therefore a SK or an ASK configuration confined in a dot tends to increase its radius in order to demagnetize the system [7, 32]. The surface charges do not depend on the in-plane magnetization and the associated dipolar interaction is identical for a SK and a ASK with the same area.

Magnetic volume charges are generated from the volume magnetization divergence. The maps of the volume charges for a SK and an ASK configuration are shown in Fig.(4). The two configurations show very different volume charges maps, which allows expecting different dipolar interactions. The SK maps presents a circular symmetry and the volume charges arise from the Néel-

like moment rotation. On the other hand, the ASK maps shows a 2-fold symmetry and the presence of Bloch-like rotations along intermediate directions ($\phi = \pi/4 + n\pi/2$). The Bloch-like rotations have zero divergence and do not produce volume magnetic charges [34]. Moreover the alternation of Néel-like moment rotations with opposite chirality, i.e. opposite moment rotation sense, produces volume magnetic charges inside the ASK with opposite signs. It can be seen as a magnetic flux closure effect that reduces the dipolar interaction in the ASK.

It is possible hence to expect a reduction of the total energy of the ASK with respect to the SK due to the difference in the distribution of volume magnetic charges. Moreover, the presence of anisotropic volume charges could deform the ASK shape.

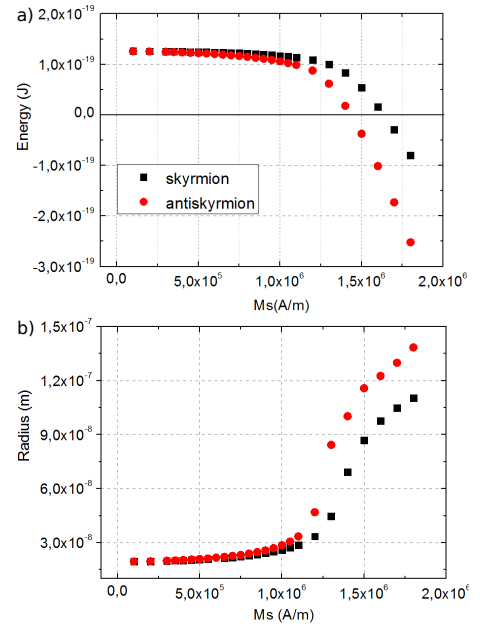


Figure 5: Energy (a) and radius (b) of a skyrmion (black) and an anti-skyrmion (red) as a function of the spontaneous magnetization M_s . The simulations are performed in circular dots of 400 nm diameter and 1 nm thickness with a fixed out-of-plane effective anisotropy K_{eff} . $A_{\text{ex}} = 16$ pJ/m $K_{\text{eff}} = 2 \cdot 10^5$ J/m³ $D = 2.0$ mJ/m²

Consequences on the stability of anti-skyrmions

To investigate in more detail the effect of the dipolar interaction on the stability and shape of SK and ASK, we studied their energy and radius as a function of the spontaneous magnetization M_s (Fig. 5). In order to consider only the effects of the volume charges and the flux closure of the surface charges we keep K_{eff} constant during the variation of M_s . Typical magnetic parameters for systems where isolated SKs have been

experimentally found are considered ($A_{\text{ex}} = 16 \text{ pJ/m}$, $K_{\text{eff}} = 2 \cdot 10^5 \text{ J/m}^3$, $D = 2.0 \text{ mJ/m}^2$) whereas M_s is varying between $0.1 \cdot 10^6 \text{ A/m}$ and $1.8 \cdot 10^6 \text{ A/m}$. In Fig. 5(a) the SK and ASK energies are considered as the energy difference between a dot with a SK or an ASK and its relative single domain state. It allows to eliminate the DMI effect on the edge magnetization [35]. Since the ASK does not present a circular shape we consider an effective radius ($r = \sqrt{\mathcal{A}/\pi}$) calculated from the area \mathcal{A} . We consider the SK and ASK \mathcal{A} as the space region where $\mathbf{m}_z > 0$. For small values of M_s the SK and the ASK are mainly stabilized by the competition between the exchange, anisotropy and DMI [29] that were shown to be equal for SK and ASK. The dipolar interaction is negligible and the SK and the ASK have comparable energy and radius. When M_s increases the dipolar interaction plays a larger role. The SK and ASK radii increase (Fig. 5(b)) allowing a more efficient flux closure between the surface magnetic charges. Both configurations gain energy but the difference in volume charges favors the ASK. For larger M_s the dipolar energy becomes comparable to the DMI energy, the total energy of the SK and the ASK decreases and their radius increases until they feel the repulsive effect from the dot edge [28]. In this regime, the SK and ASK shape and dimensions strongly depend on the symmetry and size of the microstructures in which they are confined and the volume charges become the driving force for defining the magnetic configuration. The ASK changes its shape in order to promote Bloch-like rotation. Because DMI promotes Bloch-like rotations along intermediate crystallographic directions ($\phi = \pi/4 + n\pi/2$) the ASK has the tendency to acquire a square shape (Fig. 6). Indeed this configuration allows to increase the ratio between Bloch and Néel rotations maximizing both DMI and dipolar energy gains, but increasing the DW length.

In order to quantify this tendency, we calculate the circularity factor $C = 4\pi\mathcal{A}/\mathcal{P}^2$, where \mathcal{A} is the area of the SK-ASK and \mathcal{P} the perimeter (set of point where $\mathbf{m}_z = 0$). This parameter may vary from $C_o = 1$ to $C_o = \pi/4$. The SK has a circular symmetry and this factor is should be equal to C_o . The circularity as a function of M_s for an ASK is plotted in Fig. 6. We can distinguish two different regimes. For small values of M_s the volume charges do not influence the ASK shape whereas for bigger M_s values, for which the DMI and the dipolar interaction are comparable (7), the moment rotation with an angle ($\phi = \pi/4 + n\pi/2$) is favorable and the ASK circularity decreases as a function of M_s . In Fig. 6 the SK circularity is plotted for $M_s = 1.8 \cdot 10^6 \text{ A/m}$ and for three values of the mesh size (Δx 1,2,4 nm). Note that the circularity of the SK is not the one of the circle $C_o = 1$. This is a discretization effect, i.e. a circular object discretized with a square mesh tends to assume a square shape. In order to reduce this effect we optimize the mesh size. Indeed as it is shown in Fig. 6 for a mesh

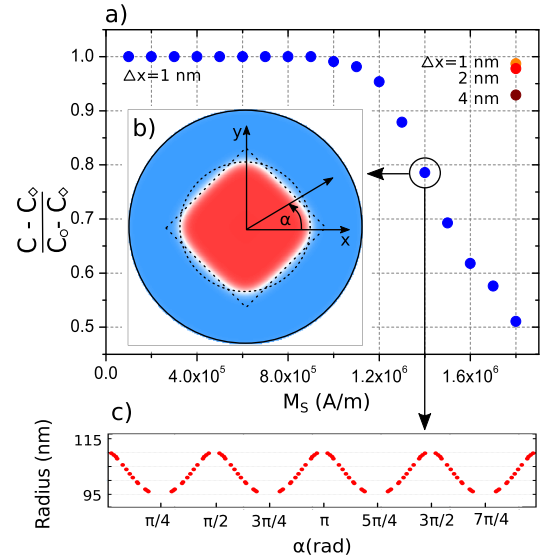


Figure 6: **(a)** Normalized circularity factor $C_n = \frac{4\pi\mathcal{A}/\mathcal{P}^2 - C_o}{C_o - C_o}$ (\mathcal{A} the area and \mathcal{P} the perimeter) for an anti-skyrmion (blue) stabilized in a dot of 400 nm as a function of M_s . The skyrmion circularity is plotted for $M_s = 1.8 \cdot 10^6 \text{ A/m}$ for three values of mesh size (Δx 1,2,4 nm)(orange, red, wine) **(b)** Magnetic configuration of an anti-skyrmion ($M_s = 1.4 \cdot 10^6 \text{ A/m}$ $A_{\text{ex}} = 16 \text{ pJ/m}$ $K_{\text{eff}} = 2 \cdot 10^5 \text{ J/m}^3$ $D = 2.0 \text{ mJ/m}^2$) with a sketch that shows the square-circular shape. **(c)** Radius of an anti-skyrmion as a function of the in-plane angle α

size of 1 nm this effect is negligible.

Finally to have a numerical confirmation of the SK and ASK stabilization mechanisms we studied the energies as a function of the SK and ASK radius for a given value of M_s . We choose $M_s = 1.2 \cdot 10^6 \text{ A/m}$ in order to study the regime where the dipolar interaction shows its effects. These simulations are performed starting from two different initial states, respectively with larger and smaller radius than the equilibrium one. We tracked the energies during the relaxation towards the equilibrium (Fig. 7(a,b)). The energy path that the SK and ASK follow during the relaxation depends on the simulation parameters. They have been optimized in order to obtain a unique correspondence between the energy behavior of the SK and ASK energies as a function of the radius and the relaxation path. We confirmed it checking that the anisotropy and the DMI energies vary linearly with the radius and are passing through the origin [29].

Upon diameter increase, anisotropy and exchange energies increase and DMI and dipolar energies decrease, all almost linearly. The balance between these terms is rather subtle as all these energies almost compensate (the absolute value of the total energy is more than one order of magnitude smaller than the absolute value of any of the separate energies). In Fig. 7(c) we show that for a given set of magnetic parameters the ASK is more stable

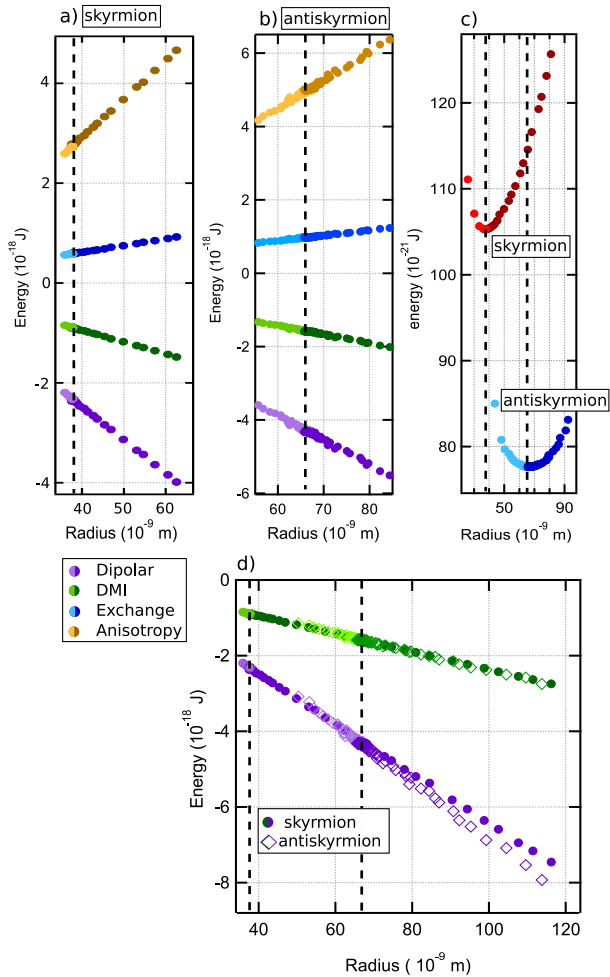


Figure 7: Magnetic energies of a skyrmion (a) and an anti-skyrmion (b) as a function of the radius for a given set of magnetic parameters ($M_s = 1.2 \cdot 10^6$ A/m $A_{\text{ex}} = 16$ pJ/m $K_{\text{eff}} = 2 \cdot 10^5$ J/m³ $D = 2.0$ mJ/m²). (c) Total energy for a skyrmion (red) and an anti-skyrmion (blue) as a function of the radius. (d) Comparison between the DMI (green) and the dipolar interaction (violet) for a skyrmion (dots) and an anti-skyrmion (squares) as a function of the radius. The vertical dotted lines in all panels correspond to the equilibrium radius of SK and/or ASK

than the SK and it has a bigger radius. It can be understood considering Fig. 7(d) where the behavior of the DMI and of the dipolar interaction energies are compared as a function of the radius. One can notice that the DMI has the same behavior for the SK and ASK, unlike the dipolar energy, which upon increasing radius decreases faster for the ASK than for the SK. This difference is the fundamental reason for the energy difference between the SK and the ASK. Even if this difference at equilibrium is not visible in the energy range shown in Fig. 7(d) it becomes fundamental in the anti-skyrmion/skyrmion energy range Fig. 7(c). Indeed the SK and ASK configurations are solutions of the competition between all the

magnetic energies and any small variation of one of the energies can imply a strong change of the SK and ASK energy and radius.

CONCLUSIONS

We have shown that when the dipolar interactions are neglected it is possible to write the ASK energy in a circular symmetric form. The SK and the ASK in systems with different symmetry but same strength of magnetic interactions have the same size and stability energy. The presence of dipolar interactions breaks the circular symmetry of the ASK energy. With the support of micromagnetic simulations we have studied the energy and the shape of SK and ASK as a function of M_s and explain the role of the dipolar interaction. We can distinguish three different effects. The interaction due to the surface charges does not break the circular symmetry and stabilizes in the same way SK and ASK. The volume charges depend on the in-plane moment configuration. While the SK configuration shows homochiral Néel moment rotation, in anti-skyrmions the rotations are partly Néel and partly Bloch rotations. The Bloch rotations do not produce magnetic charges. The ASK configuration is therefore more stable and the tendency to favor Bloch rotation induces a square shape. Moreover the presence of Néel rotations with different chirality induces a flux closure effect and helps the ASK stability. The relative difference in energy between a SK and an ASK is large. It is due to the fact that both the configurations are stable when all the magnetic energies cancel each other and a small variation of a single parameter can induce big shape and energy differences.

ACKNOWLEDGEMENTS

We want to express our thanks to Florian Dadoushi and Pieds Nus (Rémi Dupouy) for the fundamental support on the development of data analysis software and the ANR, project ANR-14-CE26-0012 (ULTRASKY), and the Laboratoire d'excellence LANEF (Grant No. ANR-10-LABX-51-01) for financial support.

* Electronic address: lorenzo.camosi@neel.cnrs.fr

† Electronic address: jan.vogel@neel.cnrs.fr

- [1] A. Bogdanov and D. Yablonskii, Zh. Eksp. Teor. Fiz. **96**, 253 (1989).
- [2] B. Ivanov, V. Stephanovich, and A. Zhudskii, J. Magn. Magn. Mater. **88**, 116 (1990).
- [3] S. Mühlbauer, B. Binz, F. Jonietz, C. Pfleiderer, A. Rosch, A. Neubauer, R. Georgii, and P. Böni, Science **323**, 915 (2009).

- [4] X. Z. Yu, Y. Onose, N. Kanazawa, J. H. Park, J. H. Han, Y. Matsui, N. Nagaosa, and Y. Tokura, *Nature* **465**, 901 (2010).
- [5] S. Heinze, K. von Bergmann, M. Menzel, J. Brede, A. Kubetzka, R. Wiesendanger, G. Bihlmayer, and S. Blügel, *Nature Phys.* **7**, 713 (2011).
- [6] W. Jiang, P. Upadhyaya, W. Zhang, G. Yu, M. B. Jungfleisch, F. Y. Fradin, J. E. Pearson, Y. Tserkovnyak, K. L. Wang, O. Heinonen, et al., *Science* **349**, 283 (2015).
- [7] O. Boulle, J. Vogel, H. Yang, S. Pizzini, D. d. S. Chaves, A. Locatelli, T. O. Montes, A. Sala, L. D. Buda-Prejbeanu, O. Klein, et al., *Nat. Nanotechnol.* **11**, 449 (2016).
- [8] I. Dzyaloshinskii, *Sov. Phys. JETP* **5**, 1259 (1957).
- [9] T. Moriya, *Phys. Rev.* **120**, 91 (1960).
- [10] L. Camosi, S. Rohart, O. Fruchart, S. Pizzini, M. Belmeguenai, Y. Roussigné, A. Stashkevich, S. M. Cherif, L. Ranno, M. de Santis, and J. Vogel, *Phys. Rev. B* **95**, 214422 (2017).
- [11] M. Hoffmann, B. Zimmermann, G. P. Mueller, D. Schuerhoff, N. S. Kiselev, C. Melcher, and S. Blügel, *Nature Comm.* **8**, 308 (2017).
- [12] N. Nagaosa and Y. Tokura, *Nat. Nanotechnol.* **8**, 899 (2013).
- [13] A. Neubauer, C. Pfleiderer, B. Binz, A. Rosch, R. Ritz, P. Niklowitz, and P. Böni, *Phys. Rev. Lett.* **102**, 186602 (2009).
- [14] Y. Li, N. Kanazawa, X. Z. Yu, A. Tsukazaki, M. Kawasaki, M. Ichikawa, X. F. Jin, F. Kagawa, and Y. Tokura, *Phys. Rev. Lett.* **110**, 117202 (2013).
- [15] J. Zang, M. Mostovoy, J. H. Han, and N. Nagaosa, *Phys. Rev. Lett.* **107**, 136804 (2011).
- [16] W. Jiang, X. Zhang, G. Yu, W. Zhang, X. Wang, M. B. Jungfleisch, J. E. Pearson, X. Cheng, O. Heinonen, K. L. Wang, et al., *Nature Phys.* **13**, 162 (2017).
- [17] K. Litzius, B. K. Ivan Lemesch, P. Bassirian, L. Caretta, K. Richter, F. Büttner, K. Sato, O. A. Tretiakov, J. Förster, R. M. Reeve, et al., *Nature Phys.* **13**, 170 (2017).
- [18] A. K. Nayak, V. Kumar, P. Werner, E. Pippel, R. Sahoo, F. Damay, U. K. Rössler, C. Felser, and S. Parkin, **548** (2017).
- [19] U. Güngördü, R. Nepal, O. A. Tretiakov, K. Belashchenko, and A. A. Kovalev, *Phys. Rev. B* **93**, 064428 (2016).
- [20] S. Huang, C. Zhou, G. Chen, H. Shen, A. K. Schmid, K. Liu, and Y. Wu, *Phys. Rev. B* **96**, 144412 (2017).
- [21] A. Thiele, *Phys. Rev. Lett.* **30**, 230 (1973).
- [22] N. Kiselev, A. Bogdanov, R. Schäfer, and U. Rössler, *Nature Commun.* **8** (2017).
- [23] K. Everschor-Sitte, M. Sitte, T. Valet, A. Abanov, and J. Sinova, *New J. Phys.* **19**, 092001 (2017).
- [24] X. Zhang, J. Xia, Y. Zhou, X. Liu, H. Zhang, and M. Ezawa, *Nature Commun.* **8** ((2017).
- [25] A. N. Bogdanov and U. K. Rössler, *Phys. Rev. Lett.* **87**, 037203 (2001).
- [26] U. Rössler, A. Bogdanov, and C. Pfleiderer, **442**, 797 (2006).
- [27] A. O. Leonov, T. L. Monchesky, N. Romming, A. Kubetzka, A. N. Bogdanov, and R. Wiesendanger, *New J. Phys.* **18**, 065003 (2016).
- [28] S. Rohart and A. Thiaville, *Phys. Rev. B* **88**, 184422 (2013).
- [29] A. Bernand-Mantel, L. Camosi, A. Wartelle, N. Rougemaille, M. Darques, and L. Ranno, *arxiv:1712.03154* (2017).
- [30] The Object Oriented MicroMagnetic Framework (OOMMF) project at ITL/NIST, URL <http://math.nist.gov/oommf/>.
- [31] Y.-O. Tu, *J. Appl. Phys.* **42**, 5704 (1971).
- [32] M. Schott, A. Bernand-Mantel, L. Ranno, S. Pizzini, J. Vogel, H. Béa, C. Baraduc, S. Auffret, G. Gaudin, and D. Givord, *Nano Letters* **17**, 3006 (2017).
- [33] K. Y. Guslienko, *IEEE Magn. Lett.* **6**, 1 (2015).
- [34] A. Thiaville, S. Rohart, E. Jué, V. Cros, and A. Fert, *Europhys. Lett.* **100**, 57002 (2012).
- [35] S. Pizzini, J. Vogel, S. Rohart, L. D. Buda-Prejbeanu, E. Jué, O. Boulle, I. M. Miron, C. K. Safeer, S. Auffret, G. Gaudin, et al., *Phys. Rev. Lett.* **113**, 047203 (2014).